Title

Resonance Raman spectra of wurtzite and zincblende CdSe nanocrystals

Journal

Chemical Physics, 422

ISSN

0301-0104

Authors

Kelley, AM
Dai, Q
Jiang, ZJ
et al.

Publication Date

2013

DOI

10.1016/j.chemphys.2012.09.029

Peer reviewed

Resonance Raman spectra of wurtzite and zincblende CdSe nanocrystals

Anne Myers Kelley,* Quanqin Dai, Zhong-jie Jiang, Joshua A. Baker, and David F. Kelley

Chemistry and Chemical Biology, School of Natural Sciences, University of California, Merced, 5200 North Lake Road, Merced, CA 95343

*Corresponding author. Tel. 209-228-4345, email amkelley@ucmerced.edu

Abstract. Resonance Raman spectra and absolute differential Raman cross-sections have been measured for CdSe nanocrystals in both the wurtzite and zincblende crystal forms at four excitation wavelengths from 457.9 to 514.5 nm. The frequency and bandshape of the longitudinal optical (LO) phonon fundamental is essentially identical for both crystal forms at each excitation wavelength. The LO phonon overtone to fundamental intensity ratio appears to be slightly higher for the wurtzite form, which may suggest slightly stronger exciton-phonon coupling from the Fröhlich mechanism in the wurtzite form. The LO fundamental Raman cross-sections are very similar for both crystal forms at each excitation wavelength.

Keywords. Semiconductor nanocrystal; electron-phonon coupling; resonance Raman

Most of the II-VI compound semiconductors (*e.g.* Zn, Cd, or Hg with S, Se, or Te) are found in one of two crystal structures near ambient temperature and pressure: wurtzite (WZ) or zincblende (ZB). These two structures are quite similar to one another, with each atom having essentially the same tetrahedral arrangement of nearest neighbors in each structure. While there have been many theoretical studies comparing various properties of different crystal forms of a given material for both III-V and II-VI semiconductors,[1-6] there are relatively few experimental comparisons for the bulk crystals. However, high quality nanocrystals of some materials can be prepared in either form by manipulating the growth conditions. For example, CdSe adopts the wurtzite structure in the bulk, but nanocrystals can be prepared in both crystal structures.[7,8] Conversely, CdTe normally has the zincblende structure in the bulk, but nanocrystals having the wurtzite structure have been reported.[9,10]

Because the two crystal structures are so similar, many of their optical, electronic, and mechanical properties are also very similar, as are the ways in which these properties are modified by quantum confinement. For example, the size-dependent optical spectra of WZ and ZB CdSe and CdTe differ only in subtle ways, and the lowest-frequency absorption maximum as a function of size is nearly the same for the two crystal structures.[11,12] One significant difference between the WZ and ZB structures is their piezoelectricity. The electromechanical tensor of a WZ crystal has a large (3,3) element, meaning that compression or expansion along the *c* axis generates a substantial electric field along that axis. In contrast, the electromechanical tensor of a ZB crystal has only smaller, off-diagonal elements. Piezoelectric effects can significantly alter the spectroscopy and dynamics of these nanocrystals. In a recent study, internal electric fields produced in part by the material's piezoelectric response were shown to have an effect on the Auger dynamics in WZ CdSe nanoparticles.[13] The differences in piezoelectricity might be expected to contribute to different magnitudes of electron-phonon

coupling in the two crystal forms, but to our knowledge this has not been explored, at least in II-VI systems.

Electron-phonon coupling in bulk semiconductors is ascribed to three principal mechanisms: deformation potential coupling, piezoelectric coupling, and Fröhlich coupling.[14] Deformation potential coupling is the variation in the electronic band energies caused by the changes in bond lengths and bond angles upon displacing the atoms. It occurs in all materials, polar or not, and can act on both acoustic and optical phonons. Deformation potential coupling is fundamentally a short-range effect in that it depends almost entirely on near-neighbor interactions. It is the dominant vibronic coupling mechanism in molecules. The bandgap deformation potentials are quite similar in WZ and ZB forms of the same material,[2,4,5,15,16] so this coupling mechanism is not expected to vary much between the two crystal forms. Piezoelectric coupling arises from the macroscopic electric field induced by strain in a noncentrosymmetric crystal. It exists only in polar crystals and acts only on acoustic phonons, in which the phonon causes macroscopic distortion of the lattice. As the largest component of the electromechanical tensor is considerably larger in WZ than in ZB crystals,[3,6,14,17] one might expect stronger coupling to acoustic phonons in WZ crystals; however, since piezoelectric coupling is a long-range effect (proportional to 1/q), its importance in small nanocrystals has been questioned.[18,19] Fröhlich coupling also exists only in polar crystals and acts on long-wavelength optical phonons that do not cause macroscopic distortion of the lattice but do produce net charge separation which generates a macroscopic electric field. Like piezoelectric coupling, it is a long-range effect that may be less important in nanocrystals than on the bulk. In a bulk semiconductor the Fröhlich Hamiltonian is proportional to $[\omega_{LO}(\varepsilon_\infty^{-1} - \varepsilon_0^{-1})]^{1/2}$ where ω_{LO} is the longitudinal optical phonon frequency, ε_∞ is the "high-frequency" dielectric constant (at frequencies above vibrational resonances but below electronic resonances), and ε_0 is the

static dielectric constant. As the difference between ε_∞ and ε_0 is expected to be larger for WZ crystals along the *c* axis than for ZB crystals, the electron-phonon coupling to optical phonons should be correspondingly larger.

In this paper we present an experimental comparison of the resonance Raman spectra of small, approximately spherical CdSe nanocrystals in both wurtzite and zincblende forms. Raman spectra have been reported for bulk ZnS in WZ and ZB forms,[20] CdS platelets and thin films containing varying amounts of both WZ and ZB structures,[21,22] nanocrystals of GaAs and InAs with different percentages of WZ and ZB structure,[23,24] and large (not quantum confined) WZ and ZB GaAs nanowires.[25,26] However, we know of no previous studies comparing the experimental phonon spectra of wurtzite and zincblende nanocrystals of any II-VI compound. Here we compare the Raman frequencies, bandshapes, and overtone intensities for WZ and ZB CdSe nanocrystals of comparable size, using excitation at several different wavelengths above the band gap. We also report what we believe to be the first values of absolute Raman scattering cross-sections for these nanocrystals.

Methods

CdSe nanocrystals in the zincblende and wurtzite crystal forms were synthesized as described in ref. [13]. The sizes of the NCs were determined from the wavelength of the lowest-energy absorption maximum using eq. (14) of ref. [27], resulting in diameters of 3.26 nm for the WZ crystals absorbing at 553 nm and 3.15 nm for the ZB crystals absorbing at 548 nm. Although the relationship in ref. [27] was developed for the WZ form, Čapek *et al*. show that the correspondence between absorption maximum and size is nearly identical for WZ and ZB crystals.[28] The nanocrystal concentrations in the spectroscopic samples were determined from their absorbances at the peak of the lowest-energy absorption band via eqs. (15) and (16) of

ref. [27], which accounts for the monodispersity of the sample through the half-width at half maximum of the low-energy side of the absorption band. While again this expression is derived for the WZ form, other studies indicate that the molar absorptivities of the two crystal forms are very similar.[28-30]

Samples for Raman spectroscopy were dissolved in cyclohexane at concentrations ranging from 6 to 21 μM. They were contained in 1 mm path length fused silica cuvettes which were placed on the stage of a Jobin-Yvon T64000 Raman microscope system consisting of a 0.64-m triple spectrograph coupled to a confocal Raman microprobe based on an Olympus BX-41 microscope with a 10X objective. Excitation at 457.9, 476.5, 496.5, and 514.5 nm was provided by a Coherent Innova 90C-5 argon-ion laser. The laser power measured at the sample was about 2.5 mW; neither the appearance of the CdSe Raman lines nor the intensity of the CdSe lines relative to those of the cyclohexane solvent were changed by reducing the power by a factor of five. The detector was a UV coated, back illuminated, liquid nitrogen cooled CCD with >70% quantum efficiency from 425-800 nm. Spectral resolution was 3-4 cm^{-1} and all spectra were obtained at ambient temperature. Typically, signal was integrated on the detector for 20 to 60 s before being read out, and 10 to 200 such integrations (10-60 minutes total) were summed to obtain the spectrum of each sample. Longer integrations were needed at 496.5 nm and particularly at 514.5 nm to reduce the shot noise from the underlying fluorescence background.

Absolute differential Raman cross-sections were determined from the integrated area of the ~206 cm^{-1} longitudinal optical (LO) phonon relative to that of the 801 cm^{-1} cyclohexane line, for which the absolute cross-section has been determined as a function of excitation wavelength.[31] Igor Pro 6.22A (Wavemetrics) was used to fit the raw data to a sum of two peaks (Gaussian and Voigt) plus a cubic background over the 125-300 cm^{-1} region, and to a

single Voigt peak plus a cubic background in the 725-875 cm^{-1} region. The absolute differential Raman cross-section for the LO phonon was then calculated as follows:

$$\left(\frac{d\sigma}{d\Omega}\right)_{CdSe} = \left(\frac{d\sigma}{d\Omega}\right)_{cyc} \left[\frac{(\alpha_L+\alpha_{LO})}{(\alpha_L+\alpha_{cyc})} \frac{\left\{1-e^{-2.303(\alpha_L+\alpha_{cyc})}\right\}}{\left\{1-e^{-2.303(\alpha_L+\alpha_{LO})}\right\}}\right] \frac{C_{cyc}}{C_{CdSe}} \frac{I_{CdSe}}{I_{cyc}} \quad (1)$$

Here $\left(\frac{d\sigma}{d\Omega}\right)_{cyc}$ is the absolute differential cross-section for the 801 cm^{-1} cyclohexane line, converted from total cross-section assuming a depolarization ratio of 0.08. C_{cyc} and C_{CdSe} are the molar concentrations in the solution (the concentration of liquid cyclohexane is 9.25 M), and I_{CdSe} and I_{cyc} are the integrated peak areas.

The quantity in square brackets corrects the observed intensities for the differential reabsorption of the backscattered Raman light at the frequencies of the LO phonon and the cyclohexane standard; α_L, α_{LO}, and α_{cyc} are the absorbances of the sample at the laser, scattered LO phonon, and scattered cyclohexane wavelengths, respectively, in the 1 mm path length of the sample cell. This equation is derived under the assumption of pure 180^o backscattering; that is, the numerical aperture of the microscope objective is ignored. The incident laser light is assumed to be attenuated following Beer's Law as the light penetrates through the sample, the amount of Raman scattered light generated at each point is proportional to the laser intensity at that point, and then the Raman scattered light leaving the sample is also attenuated according to Beer's Law. At the concentrations employed, this correction was no larger than 8% for any sample at any excitation wavelength.

For examination of the overtone to fundamental ratios, a pure cyclohexane spectrum was first subtracted from each CdSe spectrum, scaled to remove the strong 801 cm^{-1} line from the subtracted spectrum. This was needed to remove the contribution to the overtone region from the weak cyclohexane peaks at 384 and 427 cm^{-1}. Igor Pro was then used to fit and subtract a polynomial background from each spectrum in order to remove the fluorescence component.

Results and Discussion

The absorption spectra of the WZ and ZB nanocrystals are quite similar. The first absorption maximum, assigned as the $1S_e$-$1S_{3/2}$ transition, is at 548 nm for the ZB crystals and at 553 nm for the WZ crystals. The spectra differ mainly in the region just to the blue of the main absorption band, where the ZB crystals exhibit a weak, resolved band separated by about 0.18 eV from the main absorption while the WZ crystals exhibit only a shoulder about 0.13 eV to the blue of the main peak. This feature is assigned as the $1S_e$-$2S_{3/2}$ transition, and the difference in splitting between the $1S_e$-$1S_{3/2}$ and $1S_e$-$2S_{3/2}$ transitions is a well-known difference between the optical spectra of the two crystal forms.[8]

Figure 1 shows raw resonance Raman spectra of WZ and ZB CdSe nanocrystals at two excitation wavelengths. There is almost no observable fluorescence in the region of the Raman spectrum with 457.9 nm excitation, while with 514.5 nm excitation the background is quite strong, particularly for the WZ sample. This fluorescence comes from a small population of much smaller CdSe particles.

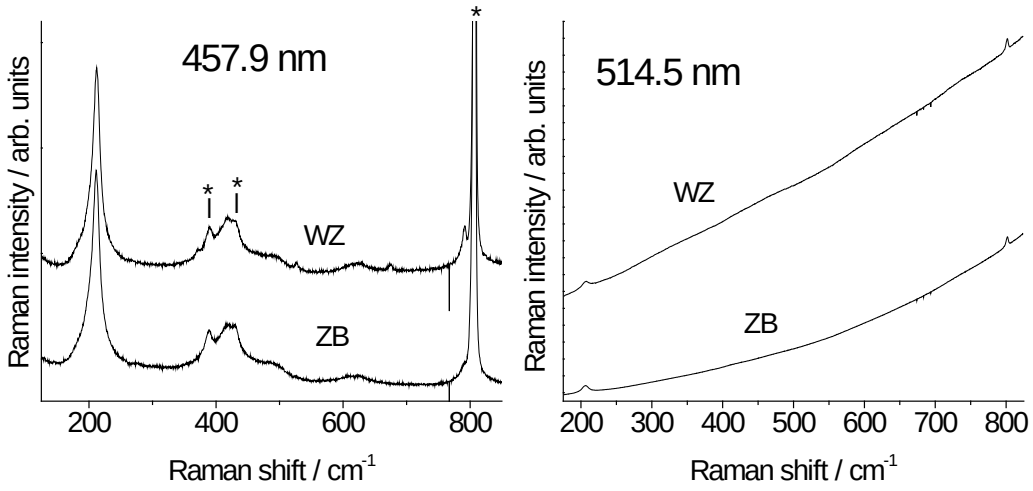

Figure 1. Raw resonance Raman spectra of ~3.2 nm diameter CdSe nanocrystals in cyclohexane in the wurtzite (WZ) and zincblende (ZB) forms. The peak near 206 cm^{-1} is the CdSe LO phonon and the peak at 801 cm^{-1} is the cyclohexane internal standard band. Weak lines at 384 and 426 cm^{-1} (asterisks) are from the cyclohexane solvent and very weak features at 522, 673, and 786 cm^{-1} in the WZ spectrum are from residual toluene. The WZ spectrum has been displaced vertically for clarity in the 457.9 nm spectrum. Nanocrystal concentrations are 12.3 μM (WZ) and 12.2 μM (ZB) at 457.9 nm, 15.8 μM (WZ) and 21.5 μM (ZB) at 514.5 nm.

Figure 2 compares the resonance Raman spectra of WZ and ZB CdSe nanocrystals in the region of the LO phonon fundamental and its first overtone at all four excitation wavelengths, following subtraction of the cyclohexane solvent spectrum and the fluorescence background. The bandshape in the LO phonon region varies somewhat with excitation wavelength, showing a broader base at shorter wavelengths, but is nearly identical for the two crystal forms at each wavelength. The peak frequency of the LO phonon fundamental is 206 ± 1 cm^{-1} for both crystal forms at each excitation wavelength. The overtone to fundamental intensity ratios are also quite similar, but the wurtzite nanocrystals appear to have slightly higher relative intensities in the overtone region based on visual inspection. These differences are also evident in the integrated

peak areas (Table 1). The bandshape and intensity of the weak, broad overtone band is very sensitive to the choice of background subtraction parameters at the longer excitation wavelengths, where there is a strong fluorescence background and no overtone intensity can be observed in the raw data. For these reasons we are unwilling to draw any conclusions about the excitation wavelength dependence of the overtone intensity.

Table 1. LO phonon overtone to fundamental ratios based on integrated intensities

Excitation wavelength / nm	wurtzite	zincblende
457.9	0.14	0.11
476.5	0.13	0.09
496.5	0.20	0.13
514.5	0.12	0.11

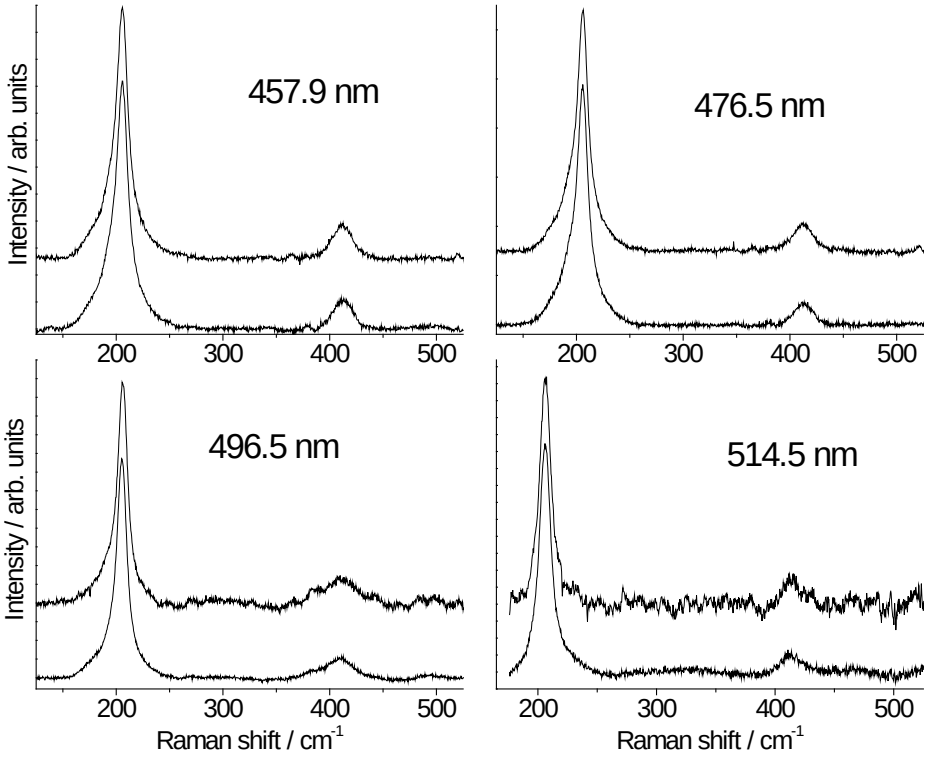

Figure 2. Background and solvent subtracted resonance Raman spectra of ~3.2 nm diameter CdSe nanocrystals in cyclohexane in the wurtzite (upper, displaced vertically) and zincblende (lower) forms. All spectra have been normalized to the LO fundamental maximum.

Figure 3 plots the differential Raman cross-section for the LO phonon fundamental for both forms at each of the four excitation wavelengths as calculated from eq. (1). The error bars represent the experimental standard deviations of 2-4 measurements taken on different days and at different concentrations, but do not include estimates of systematic errors arising from, for example, the uncertainties in the cyclohexane standard cross-sections. The absorption spectra are plotted alongside for comparison. This plot shows that the two crystal forms have very similar absolute differential Raman cross-sections, and that the Raman cross-sections for the LO phonon fundamental do not increase significantly as the absorption cross-section increases at shorter excitation wavelengths.

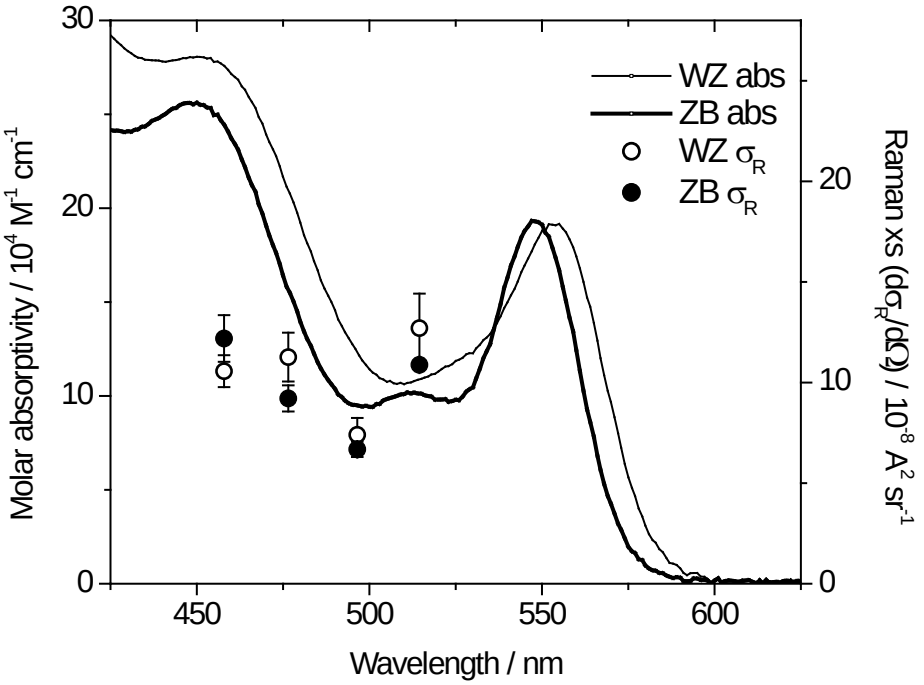

Figure 3. Molar absorptivity (lines) and differential resonance Raman cross-section for the LO phonon fundamental (points) for ~3.2 nm diameter CdSe nanocrystals in cyclohexane in the wurtzite (WZ) and zincblende (ZB) crystal forms.

The Raman spectra of the two crystal forms in the region of the LO phonon fundamental are essentially superimposable at all four excitation wavelengths used. Our data show no evidence for differences in the frequencies or relative intensities of the resonance Raman-enhanced modes for the two crystal structures. In both cases there is a fairly sharp peak at 206 cm^{-1} with at least one shoulder at lower frequencies, which becomes more apparent at shorter excitation wavelengths. This shoulder is usually assigned as a "surface optical" phonon based on continuum mechanics calculations, although atomistic simulations[32] suggest that the actual phonon mode descriptions are not so simple. Experimental and theoretical studies on the WZ and ZB forms of ZnS similarly find very similar frequencies for the optical phonons.[20,33]

Resonance Raman spectra contain information about not only the ground-state phonon frequencies but also the magnitude of exciton-phonon coupling. It is often assumed that the Huang-Rhys factor, S, may be obtained from the intensity ratio of the first overtone to the fundamental. Within the assumption of linear exciton-phonon coupling, the intensity of the $v = 0 \rightarrow v = 2$ vibronic transition, relative to the $v = 0 \rightarrow v = 1$, is given by S/2. However, the situation is more complicated in resonance Raman scattering where many different vibronic levels participate as intermediate states in the two-photon process.[34-36] While high overtone intensities do generally require strong electron-phonon coupling, the overtone to fundamental intensity ratio cannot be used directly to obtain the Huang-Rhys factor. The overtone to fundamental ratio is also influenced by the frequency of the vibration (low-frequency modes, such as the LO phonon, tend to show weaker overtones than higher-frequency modes with the same Huang-Rhys factor), excited-state dephasing rate (faster dephasing reduces overtone intensities), presence of other vibronically active vibrations, and constructive or destructive interferences among multiple overlapping electronic transitions contributing to the resonance enhancement. Accurate determination of exciton-phonon coupling strengths from resonance Raman intensities generally requires detailed modeling of the ground- and excited-state structure and dynamics, constrained by both absolute scattering cross-sections and the electronic absorption spectrum.[34-36] In view of the relatively close similarity between the electronic spectra of WZ and ZB nanocrystals, it is probably reasonable to ascribe the slightly higher overtone intensities in the wurtzite form to slightly stronger exciton-phonon coupling. However, numerical simulations of the spectra need to be carried out to exclude other explanations.

In one previous study comparing exciton-phonon coupling in WZ and ZB GaN epilayers, Xu *et al*. concluded from the temperature dependence of the exciton luminescence linewidth

that the exciton-phonon coupling is about twice as large in the zincblende form as in the wurtzite form.[37] However, even for a given crystal form (wurtzite CdSe nanocrystals), efforts to measure the strength of exciton-phonon coupling have resulted in no consensus on either the magnitude of the Huang-Rhys factors or their size dependence, with S values varying by nearly two orders of magnitude for particles of similar size and general morphology depending on method of preparation and the experimental technique employed.[38] Values based on overtone intensities in resonance Raman spectra are often higher than those derived from other experimental methods, leading to the suggestion that many resonance Raman measurements are influenced by photoinduced charging or other changes caused by prolonged irradiation of often solid-phase samples. Accumulation of trapped charges, usually at the surface of the nanocrystal, has also been implicated as a confounding factor in a number of photophysical processes including multiple exciton generation,[39-43] luminescence blinking,[42,43] and dynamics of excitons and multiexcitons.[13,43,44] Literature values for the intensity ratio I_{2LO}/I_{LO} for CdSe nanoparticles in the 2-5 nm diameter size range, under varying excitation conditions, are mostly in the range from 0.2-0.4.[45-48] Our values of 0.15 to 0.2 for the wurtzite form are on the low end of this range and we observed no power dependence of our spectra, suggesting that these values represent intrinsic properties of the nanocrystal.

Although relative Raman excitation profiles for CdSe nanocrystals have been published before,[47] to our knowledge absolute Raman cross-sections have been reported only for CdS nanoclusters.[49] The total Raman cross-section for the CdS LO phonon fundamental, measured near the peak of the lowest-energy absorption band, was found to be 2-4 x 10^{-6} Å^2 for 3-7 nm diameter particles at room temperature. These total cross sections correspond, assuming a depolarization ratio of 1/3, to a differential Raman cross-section of 2-4 x 10^{-7} Å^2. These are several times larger than the values we measure for 3.2 nm diameter CdSe particles at 300 K

using excitation to the blue of the first absorption band. In the CdS work, the particles studied had very little fluorescence so it was possible to scan the excitation through the entire lowest-energy transition, which was in the 440-470 nm region for the CdS particles used. Our CdSe nanocrystals have few defects and exhibit strong fluorescence, making it impossible to detect Raman scattering when exciting near the first absorption maximum, where we might expect to observe higher Raman cross-sections.

The absolute Raman cross-sections for both crystal forms are nearly the same at 514.5 nm and 457.9 nm excitation although the absorption cross-sections are more than a factor of two greater at the shorter wavelength. More recent measurements on wurtzite NCs, using samples that have better monodispersity as evidenced by a clearly resolved $1S_e$-$2S_{3/2}$ transition, show smaller Raman cross-sections in the 514.5 to 496.5 nm range but also show a large increase at 532 and 543.5 nm (experiments performed on samples whose fluorescence has been quenched by adding hole accepting surface ligands.) Previously reported relative Raman excitation profiles also showed a pronounced diminution on the high-energy side of the first excitonic absorption band.[49,50] As resonance Raman cross-sections scale as the square of the oscillator strength for the resonant transition, one would generally expect stronger Raman scattering at shorter excitation wavelengths where the absorbance is higher. Several explanations can be proposed for the weaker than expected scattering: the electron-phonon coupling may be smaller for the higher-energy excitations,[46] electronic dephasing and/or population decay may be faster at higher energies,[34-36] or contributions from multiple overlapping resonant states at higher energies may interfere destructively in the resonance Raman amplitude.[36] Distinguishing among these possibilities will require additional experimental results and detailed simulations of the absorption spectra and excitation profiles,[35,36] currently underway. Interestingly, low-temperature photoluminescence excitation (PLE) spectra were

found to show much more structure than the absorbance at shorter wavelengths,[51] although subsequent literature reports disagree on this point.[52,53] Understanding the dynamics of these higher excited states is central for assessing the feasibility of multiple exciton generation, hot carrier transfer, and other technologically important processes.

Acknowledgments

This work was supported by NSF grant CHE-1112192.

[1] S. Duman, A. Sütlü, S. Bagci, H. M. Tütüncü, and G. P. Srivastava, "Structural, elastic, electronic, and phonon properties of zinc-blende and wurtzite BeO", J. Appl. Phys. **105,** 033719 (2009).

[2] J.-H. Yang, S. Chen, W.-J. Yin, X. G. Gong, A. Walsh, and S.-H. Wei, "Electronic structure and phase stability of MgTe, ZnTe, CdTe, and their alloys in the *B*3, *B*4, and *B*8 structures", Phys. Rev. B **79,** 245202 (2009).

[3] K. Shimada, T. Sota, and K. Suzuki, "First-principles study on electronic and elastic properties of BN, AlN, and GaN", J. Appl. Phys. **84,** 4951-4958 (1998).

[4] T. Cheiwchanchamnangij and W. R. Lambrecht, "Band structure parameters of wurtzite and zinc-blende GaAs under strain in the GW approximation", Phys. Rev. B **84,** 035203 (2011).

[5] Y. Z. Zhu, G. D. Chen, H. Ye, A. Walsh, C. Y. Moon, and S.-H. Wei, "Electronic structure and phase stability of MgO, ZnO, CdO, and related ternary alloys", Phys. Rev. B **77,** 245209 (2008).

[6] M. Catti, Y. Noel, and R. Dovesi, "Full piezoelectric tensors of wurtzite and zinc blende ZnO and Zn by first-principles calculations", J. Phys. Chem. Solids **64,** 2183-2190 (2003).

[7] J. Huang, M. V. Kovalenko, and D. V. Talapin, "Alkyl Chains of Surface Ligands Affect Polytypism of CdSe Nanocrystals and Play an Important Role in the Synthesis of Anisotropic Nanoheterostructures", J. Amer. Chem. Soc. **132,** 15866-15868 (2010).

[8] M. B. Mohamed, D. Tonti, A. Al-Salman, A. Chemseddine, and M. Chergui, "Synthesis of High Quality Zinc Blende CdSe Nanocrystals", J. Phys. Chem. B **109,** 10533-10537 (2005).

[9] W. W. Yu, A. Wang, and X. Peng, "Formation and Stability of Size-, Shape-, and Structure-Controlled CdTe Nanocrystals: Ligand Effects on Monomers and Nanocrystals", Chem. Mater. **15,** 4300 (2003).

[10] H. Shen, H. Wang, X. Chen, J. Z. Niu, W. Xu, X. M. Li, X.-D. Jiang, Z. Du, and L. S. Li, "Size- and Shape-Controlled Synthesis of CdTe and PbTe Nanocrystals Using Tellurium Dioxide as the Tellurium Precursor", Chem. Mater. **22,** 4756-4761 (2010).

[11] O. Chen, Y. Yang, T. Wang, H. Wu, C. Niu, J. Yang, and Y. C. Cao, "Surface-Functionalization-Dependent Optical Properties of II-VI Semiconductor Nanocrystals", J. Am. Chem. Soc. **133,** 17504-17512 (2011).

[12] Y. A. Yang, H. Wu, K. R. Williams, and Y. C. Cao, "Synthesis of CdSe and CdTe Nanocrystals without Precursor Injection", Angew. Chem. Eng. Ed. **44,** 6712-6715 (2005).

[13] Z. Jiang and D. F. Kelley, "Surface Charge and Piezoelectric Fields Control Auger Recombination in Semiconductor Nanocrystals", Nano Lett. **11,** 4067-4073 (2011).

[14] P. Y. Yu and M. Cardona, *Fundamentals of Semiconductors*, Third ed. (Springer-Verlag, Berlin Heidelberg New York, 2001).

[15] M. Durandurdu, "Pressure-induced phase transition in wurtzite ZnS: An *ab initio* constant pressure study", J. Phys. Chem. Solids **70,** 645-649 (2009).

[16] P. Rinke, M. Winkelnkemper, A. Qteish, D. Bimberg, J. Neugebauer, and M. Scheffler, "Consistent set of band parameters for the group-II nitrides AlN, GaN, and InN", Phys. Rev. B **77,** 075202 (2008).

[17] J. Xin, Y. Zheng, and E. Shi, "Piezoelectricity of zinc-blende and wurtzite structure binary compounds", Appl. Phys. Lett. **91,** 112902 (2007).

[18] T. Takagahara, "Electron-phonon interactions and excitonic dephasing in semiconductor nanocrystals", Phys. Rev. Lett. **71,** 3577-3580 (1993).

[19] Q. Zhang, J. Zhang, M. I. B. Utama, B. Peng, M. de la Mata, J. Arbiol, and Q. Xiong, "Exciton-phonon coupling in individual ZnTe nanorods studied by resonant Raman spectroscopy", Phys. Rev. B **85,** 085418 (2012).

[20] O. Brafman and S. S. Mitra, "Raman Effect in Wurtzite- and Zinc-Blende-Type ZnS Single Crystals", Phys. Rev. **171,** 931-934 (1968).

[21] T. T. K. Chi, G. Gouadec, P. Colomban, G. Wang, L. Mazerolles, and N. Q. Liem, "Off-resonance Raman analysis of wurtzite CdS ground to the nanoscale: structural and size-related effects", J. Raman Spectrosc. **42,** 1007-1015 (2011).

[22] R. Lozada-Morales, O. Zelaya-Angel, S. Jimenez-Sandoval, and G. Torres-Delgado, "Extra Raman modes in CdS during cubic to hexagonal structural transformation", J. Raman Spectrosc. **33,** 460-465 (2002).

[23] I. Zardo, S. Conesa-Boj, F. Peiro, J. R. Morante, J. Arbiol, E. Uccelli, G. Abstreiter, and A. Fontcuberta i Morral, "Raman spectroscopy of wurtzite and zinc-blende GaAs nanowires: Polarization dependence, selection rules, and strain effects", Phys. Rev. B **80,** 245324 (2009).

[24] J. K. Panda, A. Roy, A. Singha, M. Gemmi, D. Ercolani, V. Pellegrini, and L. Sorba, "Raman sensitivity to crystal structure in InAs nanowires", Appl. Phys. Lett. **100,** 143101 (2012).

[25] B. Ketterer, M. Heiss, E. Uccelli, J. Arbiol, and A. Fontcuberta i Morral, "Untangling the Electron Band Structure of Wurtzite GaAs Nanowires by Resonant Raman Spectroscopy", ACS Nano **5,** 7585-7592 (2011).

[26] W. Peng, F. Jabeen, B. Jusserand, J. C. Harmand, and M. Bernard, "Conduction band structure in wurtzite GaAs nanowires: A resonant Raman scattering study", Appl. Phys. Lett. **100,** 073102 (2012).

[27] J. Jasieniak, L. Smith, J. van Embden, P. Mulvaney, and M. Califano, "Re-examination of the size-dependent absorption properties of CdSe quantum dots", J. Phys. Chem. C **113,** 19468-19474 (2009).

[28] R. K. Capek, I. Moreels, K. Lambert, D. De Muynck, Q. Zhao, A. Van Tomme, F. Vanhaecke, and Z. Hens, "Optical properties of zincblende cadmium selenide quantum dots", J. Phys. Chem. C **114,** 6371-6376 (2010).

[29] C. de Mello Donegá and R. Koole, "Size dependence of the spontaneous emission rate and absorption cross section of CdSe and CdTe quantum dots", J. Phys. Chem. C **113,** 6511-6520 (2009).

[30] W. W. Yu, L. Qu, W. Guo, and X. Peng, "Experimental determination of the extinction coefficient of CdTe, CdSe, and CdS nanocrystals", Chem. Mat. **15,** 2854-2860 (2003).

[31] M. O. Trulson and R. A. Mathies, "Raman cross section measurements in the visible and ultraviolet using an integrating cavity: Application to benzene, cyclohexane, and cacodylate", J. Chem. Phys. **84,** 2068-2074 (1986).

[32] A. M. Kelley, "Electron-phonon coupling in CdSe nanocrystals from an atomistic phonon model", ACS Nano **5,** 5254-5262 (2011).

[33] Y. C. Cheng, C. Q. Jin, F. Gao, X. L. Wu, W. Zhong, S. H. Li, and P. K. Chu, "Raman scattering study of zinc blende and wurtzite ZnS", J. Appl. Phys. **106,** 123505 (2009).

[34] A. M. Kelley, "Resonance Raman and resonance hyper-Raman intensities: Structure and dynamics of molecular excited states in solution", J. Phys. Chem. A **112,** 11975-11991 (2008).

[35] A. B. Myers, "Excited electronic state properties from ground-state resonance Raman intensities", in *Laser Techniques in Chemistry*, edited by A. B. Myers and T. R. Rizzo (Wiley, New York, 1995), pp. 325-384.

[36] A. B. Myers, "Resonance Raman intensity analysis of excited-state dynamics", Acc. Chem. Res. **30,** 519-527 (1997).

[37] S. J. Xu, L. X. Zheng, S. H. Cheung, M. H. Xie, S. Y. Tong, and H. Yang, "Comparative study on the broadening of exciton luminescence linewidth due to phonon in zinc-blende and wurtzite GaN epilayers", Appl. Phys Lett. **81,** 4389-4391 (2002).

[38] A. M. Kelley, "Electron−phonon coupling in CdSe nanocrystals", J. Phys. Chem. Lett. **1,** 1296–1300 (2010).

[39] J. A. McGuire, M. Sykora, I. Robel, L. A. Padilha, J. Joo, J. M. Pietryga, and V. I. Klimov, "Spectroscopic signatures of photocharging due to hot-carrier transfer in solutions of semiconductor nanocrystals under low-intensity ultraviolet excitation", ACS Nano **4,** 6087-6097 (2010).

[40] J. A. McGuire, M. Sykora, J. Joo, J. M. Pietryga, and V. I. Klimov, "Apparent versus true carrier multiplication yields in semiconductor nanocrystals", Nano Lett. **10,** 2049-2057 (2010).

[41] A. G. Midgett, H. W. Hillhouse, B. K. Hughes, A. J. Nozik, and M. C. Beard, "Flowing versus static conditions for measuring multiple exciton generation in PbSe quantum dots", J. Phys. Chem. C **114,** 17486-17500 (2010).

[42] S. Li, M. L. Steigerwald, and L. E. Brus, "Surface States in the Photoionization of High-Quality CdSe Core/Shell Nanocrystals", ACS Nano **3,** 1267-1273 (2009).

[43] P. Kambhampati, "Hot Exciton Relaxation Dynamics in Semiconductor Quantum Dots: Radiationless Transitions on the Nanoscale", J. Phys. Chem. C **115,** 22089–22109 (2011).

[44] Z. Jiang and D. F. Kelley, "Role of Surface States in the Exciton Dynamics in CdSe Core and Core/Shell Nanorods`", J. Phys. Chem. C **114,** 17519-17528 (2010).

[45] V. M. Dzhagan, M. Y. Valakh, A. E. Raevskaya, A. L. Stroyuk, S. Y. Kuchmiy, and D. R. T. Zahn, "Size effects on Raman spectra of small CdSe nanoparticles in polymer films", Nanotechnology **19,** 305707 (2008).

[46] D. M. Sagar, R. R. Cooney, S. L. Sewall, E. A. Dias, M. M. Barsan, I. S. Butler, and P. Kambhampati, "Size dependent, state-resolved studies of exciton-phonon couplings in strongly confined semiconductor quantum dots", Phys. Rev. B **77,** 235321 (2008).

[47] A. P. Alivisatos, T. D. Harris, P. J. Carroll, M. L. Steigerwald, and L. E. Brus, "Electron-vibration coupling in semiconductor clusters studied by resonance Raman spectroscopy", J. Chem. Phys. **90,** 3463-3468 (1989).

[48] A. V. Baranov, Y. P. Rakovich, J. F. Donegan, T. S. Perova, R. A. Moore, D. V. Talapin, A. L. Rogach, Y. Masumoto, and I. Nabiev, "Effect of ZnS shell thickness on the phonon spectra in CdSe quantum dots", Phys. Rev. B **68,** 165306 (2003).

[49] J. J. Shiang, S. H. Risbud, and A. P. Alivisatos, "Resonance Raman studies of the ground and lowest electronic excited state in CdS nanocrystals", J. Chem. Phys. **98,** 8432-8442 (1993).

[50] A. P. Alivisatos, T. D. Harris, L. E. Brus, and A. Jayaraman, "Resonance Raman scattering and optical absorption studies of CdSe microclusters at high pressure", J. Chem. Phys. **89,** 5979-5982 (1988).

[51] D. J. Norris and M. G. Bawendi, "Measurement and assignment of the size-dependent optical spectrum in CdSe quantum dots", Phys. Rev. B **53,** 16338-16346 (1996).

[52] X. Peng, M. C. Schlamp, A. V. Kadavanich, and A. P. Alivisatos, "Epitaxial Growth of Highly Luminescent CdSe/CdS Core/Shell Nanocrystals with Photostability and Electronic Accessibility", J. Am. Chem. Soc. **119,** 7019 (1997).

[53] D. Tonti, F. van Mourik, and M. Chergui, "On the Excitation Wavelength Dependence of the Luminescence Yield of Colloidal CdSe Quantum Dots", Nano Lett. **4,** 2483-2487 (2004).